

Optimal synthesis of six-bar function generators

Saurav Agarwal* Jaideep Badduri† Sandipan Bandyopadhyay‡
Indian Institute of Technology Madras, Chennai, India

Abstract—This paper introduces a new approach for the synthesis of planar six-bar mechanisms via multi-objective numerical optimisation. Using the input-output relationship of such a mechanism, the structural error is formulated. In addition to the structural error, its derivative is also included in the objectives, leading to results which are comparable in accuracy to the exact methods reported in existing literature, and better than the optimisation-based methods. Also, analytical conditions are derived for the identification of the candidate designs which are free of singularities, mobility or branch defects. The formulation and results are demonstrated in the context of a Stephenson-III mechanism, though these can be generalised to the six-bar mechanisms of other topologies.

Keywords: Six-bar mechanisms, Mobility, Function generation, Double dwell

I. Introduction

This paper focuses on the development of mathematical formulations that allow the synthesis of planar six-bar mechanisms for the purpose of function generation. In particular, new developments are reported with regard to (a) assembly and mobility criteria for (a specific type of) six-bar mechanisms, (b) formalisation and utilisation of a *scalar* input-output relationship (similar to the Freudenstein's approach in the case of the planar four-bar mechanism), and (c) introducing the concept of *dual order* structural error minimisation via multi-objective optimisation.

Traditionally, four-bar mechanisms are used for the purpose of mechanical function generators, following, e.g., the *precision point* approach introduced by Freudenstein [1]. Four-bar mechanisms possess only three independent link ratios (i.e., design variables), and hence they can match an arbitrary desired output function *exactly* at the most only at three points. In comparison, the six-bar mechanisms have larger design spaces—the Stephenson-II and III can be used as function generators and have 11 architecture parameters each, whereas the Watt-II has 9 such parameters.

Naturally, the six-bar mechanisms have better potential in terms of accuracy, more so while approximating highly non-linear functions that require larger numbers of precision points to describe them closely over the desired finite interval of crank motion. This fact was recognised quite early, and there are sporadic instances of develop-

ment of such mechanisms as far back as 1940 [2]. However, not many applications and/or theoretical developments have been reported in this regard. Very recently, an *exact* synthesis of six-bar mechanisms for function generation has been carried using 8 precision points [3]. The resulting equations, if reduced to a *univariate polynomial*, would have had a total degree of 705432, which would have been practically impossible to solve accurately, even if it could be derived. Hence the set of equations were solved using a *homotopy*-based numerical method, implemented in the special purpose software, *Bertini* [4], leading to 92736 non-singular and non-degenerate real solutions.

While such a study is of great kinematic significance, it demands a great amount of effort in terms of mathematical formulation and numerical solution, not to mention the use of very specialised computational tools. Additionally, post-synthesis design validations are required to detect issues relating to assembly, mobility, and kinematic branching. An alternative approximate approach, namely, numerical optimisation, can be applied to such situations, which can make use of simpler formulations, and more generic computational tools, while producing results which are constrained *a priori* to satisfy the requirements listed above, and potentially more. In the case of the four-bar, several such studies have been reported (see, e.g., [5], [6]) for the coupler-curve synthesis problem, even after the nine-point synthesis problem was solved exactly [7]. In the case of the problem at hand, i.e., kinematic synthesis of six-bar mechanisms for function generation, however, the authors were not able to trace a single report pertaining to the optimisation approach. This may be attributed to the fact that the kinematic formulations of either the objectives or the constraint functions are not available for the six-bar mechanisms (to the best of the knowledge of the authors). For instance, a function generator would need to be free of singularities, at least in the desired range of the input. It is hard to incorporate such a requirement in the optimisation process, as no “Grashof-like” [8] analytical criterion on the design parameters exist for the case of the six-bar mechanisms.

The present work proposes an optimisation approach to the problem of design of six-bar function generators. It builds upon several new results relating to the assembly criteria, as well as full-cycle mobility. These new developments allow the identification of combinations of design variables leading to feasible mechanisms with accuracy and certainty, requiring relatively less computation involving

*agr.saurav1@gmail.com

†jaiideep.badduri@gmail.com

‡sandipan@iitm.ac.in (corresponding author)

the architecture parameters alone, and hence support the design process in a significant way.

The formulation of the problem in this work starts with the elimination of the unknown joint variables from the loop-closure equations, till only the desired output variable remains. Solution of this scalar univariate equation (termed as the FKU, following [9]) leads to the kinematic branches of the mechanism. The branches are identified using the singularity functions, which are derived following the analysis of the constraint Jacobian matrices, as shown in [10]. Each branch is studied independently to identify a potential solution in it, and also alleviating the branch-error problem in the process. The singularity conditions are converted to polynomials in an algebraic variable related to the crank motion. Characterisation of the roots of these polynomials leads to the identification of the *singularity-free* mechanisms, possessing full-cycle mobility. The problem of assembly constraints is also solved similarly, leading to the identification of link geometries capable of assembling into the mechanism at a nominal computational expense. Finally, the *structural error*, to be minimised in the optimisation process, is defined in a novel manner. The deviation in the output function is treated as the *zeroth-order* error, and its derivative, the *first-order* error, is also considered simultaneously, in what may be called a *dual order* formulation. As the latter objective aids the former, the final results obtained are typically better than in the traditional methods, wherein only the zeroth-order structural errors are considered. For the solution of the problem formulated thus, a Genetic Algorithm (GA)-based optimiser, namely NSGA-II [11], has been used. Such an optimiser is ideally suited for the problem at hand, since it handles multi-objective problems; performs global exploration, and hence does not require a “good” initial guess; furthermore, is relatively insensitive to the dimension of the design space—which allows the complete exploitation of the potential of the mechanism, that is not possible yet in the exact approaches due to the stiff rise in the computational complexity with each additional variable utilised.

In this paper, the Stephenson-III mechanism is used in all the formulations and examples, using 9 of the total of 11 variables that can be considered, as opposed to 8 in [3]. Two numerical examples are chosen from existing reports, allowing a quantitative comparison of the results achieved, which validates the efficacy of the proposed approach. It may also be noted, while this paper focuses only on the Stephenson-III, the approach can be easily adopted to any of the other six-bar mechanism topologies.

The rest of the paper is organised as follows: formulation of the mobility criteria, using assembly and singularity conditions, is described in Section II. Formalisation of the function generation problem with dual order objectives is done in Section III. The numerical studies for two function generation problems—parabola function [12], [3], and double dwell [13], [14]—and the corresponding results are pre-

sented in Section IV. Finally, the conclusions are presented in Section V.

II. Formulation: mobility criteria

A mechanism is said to possess *full-cycle mobility* if (1) assembly of the mechanism is possible for the given architecture parameters, and (2) there is no singularity, for a complete rotation of the crank. Analysis of the loop-closure equations can lead to specific conditions, e.g., Grashof’s condition [8] in the case of four-bar mechanism. Similar analysis is carried out for the six-bar mechanism of Stephenson-III type.

A. Forward kinematics

A n -degree-of-freedom mechanism has ‘ n ’ independent (or input) variables organised in the vector $\theta \in \mathbb{R}^n$. The m -dependent (or passive variables) are denoted by $\phi \in \mathbb{R}^m$. The dependent variables are related to the independent variables via ‘ m ’ scalar loop-closure constraint equations. For a one-degree-of-freedom mechanism, the loop-closure equations can be written as:

$$\eta(\theta, \phi) = \mathbf{0}. \quad (1)$$

In general, it is possible to eliminate $(m - 1)$ passive variables from the loop-closure equations to obtain a univariate in the remaining passive variable, say ϕ_m , with coefficients in terms of architecture parameters and the input variable, θ . This univariate equation has been termed as the *forward kinematics univariate* (FKU) [9] equation and can be written as:

$$f(\phi_m) = 0. \quad (2)$$

In order to obtain the *velocity coefficient* (see, e.g., [14]) of the output variable with respect to the input variable, the FKU, given in Eq. (2), is differentiated with respect to time:

$$\frac{\partial f}{\partial \theta} \dot{\theta} + \frac{\partial f}{\partial \phi_m} \dot{\phi}_m = 0. \quad (3)$$

The velocity coefficient of ϕ_m w.r.t. θ is given by:

$$K_{\phi_m \theta} = \dot{\phi}_m / \dot{\theta}. \quad (4)$$

From Eq. (3):

$$\dot{\phi}_m = - \left(\frac{\partial f}{\partial \theta} \right) / \left(\frac{\partial f}{\partial \phi_m} \right) \dot{\theta}. \quad (5)$$

Comparing Eq. (4) with Eq. (5) the velocity coefficient is given by:

$$K_{\phi_m \theta} = - \left(\frac{\partial f}{\partial \theta} \right) / \left(\frac{\partial f}{\partial \phi_m} \right), \quad (6)$$

where $\left(\frac{\partial f}{\partial \phi_m} \right) \neq 0$ at a non-singular configuration. The velocity coefficient, $K_{\phi_m \theta}$ is a rational function of ϕ_m , θ , and the architecture parameters of the mechanism.

A.1 Position kinematics of Stephenson-III mechanism

The six-bar mechanism of type Stephenson-III, shown in Fig. 1, is used to illustrate the above theories. The formulation can be extended to other types of six-bar mechanism. The input angle, θ_1 , is associated with link l_1 . The

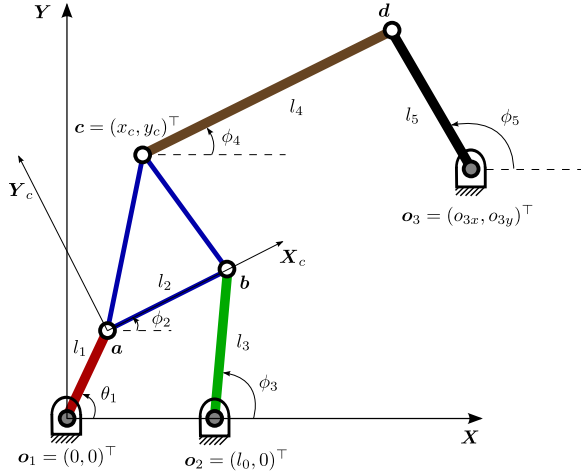


Fig. 1. Stephenson-III mechanism. The fixed pivots are denoted by \mathbf{o}_1 , \mathbf{o}_2 , and \mathbf{o}_3 . The coupler point $\mathbf{c} = (x_c, y_c)^T$ is specified with respect to the coupler's coordinate frame $(X_c Y_c)$. The input angle (θ_1) and the output angle (ϕ_5) are associated with the links l_1 and l_5 , respectively.

passive joint angles are $\phi = (\phi_2, \phi_3, \phi_4, \phi_5)^T$. The output angle ϕ_5 is associated with the link l_5 . The points $\mathbf{o}_1 = (0, 0)^T$, $\mathbf{o}_2 = (l_0, 0)^T$, and $\mathbf{o}_3 = (o_{3x}, o_{3y})^T$ are the fixed pivots of the mechanism. Point \mathbf{c} is the coupler point and its coordinates in the local frame, $X_c Y_c$, of the coupler link is given by $(x_c, y_c)^T$. For the four-bar loop $\mathbf{o}_1 \mathbf{a} \mathbf{b} \mathbf{o}_2 \mathbf{o}_1$, the constraint equations can be written as:

$$\eta_1 = l_1 \cos \theta_1 + l_2 \cos \phi_2 - l_0 - l_3 \cos \phi_3 = 0, \quad (7)$$

$$\eta_2 = l_1 \sin \theta_1 + l_2 \sin \phi_2 - l_3 \sin \phi_3 = 0. \quad (8)$$

Similarly, for the five-bar loop $\mathbf{o}_1 \mathbf{a} \mathbf{c} \mathbf{d} \mathbf{o}_3 \mathbf{o}_1$ the constraint equations can be written as:

$$\begin{aligned} \eta_3 &= l_1 \cos \theta_1 + x_c \cos \phi_2 - y_c \sin \phi_2 + l_4 \cos \phi_4 \\ &\quad - b_{3x} - l_5 \cos \phi_5 = 0, \end{aligned} \quad (9)$$

$$\begin{aligned} \eta_4 &= l_1 \sin \theta_1 + x_c \sin \phi_2 + y_c \cos \phi_2 + l_4 \sin \phi_4 \\ &\quad - b_{3y} - l_5 \sin \phi_5 = 0. \end{aligned} \quad (10)$$

The constraint equations, Eqs. (7-10), can be compactly written as:

$$\boldsymbol{\eta} = (\eta_1, \eta_2, \eta_3, \eta_4)^T = \mathbf{0}. \quad (11)$$

The following steps are employed to obtain the FKU:

- The Eqs. (7,8) are linear in the sine and cosine of ϕ_3 . Hence, the variable ϕ_3 is eliminated by finding $\cos \phi_3$ and $\sin \phi_3$, and using the trigonometric identity $\cos^2 \phi_k + \sin^2 \phi_k = 1$, to obtain the equation:

$$g_1(\theta_1, \phi_2) = 0. \quad (12)$$

- Similarly, the Eqs. (9,10) are linear in the sine and cosine of ϕ_4 . The variable ϕ_4 is eliminated as above to obtain the equation:

$$g_2(\theta_1, \phi_2, \phi_5) = 0. \quad (13)$$

- The functions g_1 and g_2 , given in Eq. (12) and Eq. (13), respectively, are linear in the sine and cosine of ϕ_2 . The variable ϕ_2 is eliminated to obtain the FKU equation:

$$g_3(\theta_1, \phi_5) = 0. \quad (14)$$

- The function g_3 can be converted into a polynomial using the standard tangent half-angle substitution $t_5 = \tan \frac{\phi_5}{2}$:

$$g_4(\theta_1, t_5).$$

The coefficients of the polynomial g_4 are functions of architecture parameters and input angle, θ_1 .

The derivation of the FKU can be described schematically as in (15).

$$\left. \begin{aligned} \eta_1(\theta_1, \phi_2, \phi_3) = 0 \\ \eta_2(\theta_1, \phi_2, \phi_3) = 0 \end{aligned} \right) \xrightarrow{\times \phi_3} g_1(\theta_1, \phi_2) = 0 \quad \left. \begin{aligned} \eta_3(\theta_1, \phi_2, \phi_4, \phi_5) = 0 \\ \eta_4(\theta_1, \phi_2, \phi_4, \phi_5) = 0 \end{aligned} \right) \xrightarrow{\times \phi_4} g_2(\theta_1, \phi_2, \phi_5) = 0 \quad \left. \begin{aligned} \xrightarrow{\times \phi_2} g_3(\theta_1, \phi_5) = 0 \\ \xrightarrow{\phi_5 \rightarrow t_5} g_4(\theta_1, t_5) = 0. \end{aligned} \right) \quad (15)$$

Here, $\xrightarrow{\times v}$ denotes elimination of the variable v . The transformation of trigonometric functions of the angle to its equivalent tangent half-angle form is represented by $\xrightarrow{\phi_5 \rightarrow t_5}$.

A.2 First order kinematics of Stephenson-III mechanism

The velocity coefficient for Stephenson-III mechanism is obtained using Eq. (6) and Eq. (14):

$$K_{\phi_5\theta_1} = - \left(\frac{\partial g_3}{\partial \theta_1} \right) / \left(\frac{\partial g_3}{\partial \phi_5} \right). \quad (16)$$

The velocity coefficient, $K_{\phi_5\theta_1}$, can be expressed as a rational function in t_5 :

$$K_{\phi_5\theta_1}(\theta_1, \phi_5) \xrightarrow{\phi_5 \rightarrow t_5} K_{t_5\theta_1}(\theta_1, t_5). \quad (17)$$

The coefficients of the rational function, $K_{t_5\theta_1}$ are functions of the architecture parameters and the input angle, θ_1 .

B. Singularity criteria of Stephenson-III mechanism

Singularity of a mechanism can be studied via the constraint Jacobian matrix of the mechanism [10]. Finding the partial derivatives of the loop-closure equations, η given in Eq. (11), with respect to ϕ gives the constraint Jacobian matrix:

$$\mathbf{J}_{\eta\phi} = \frac{\partial \eta(\theta_1, \phi)}{\partial \phi}. \quad (18)$$

Singularity occurs when the determinant of the matrix, $\mathbf{J}_{\eta\phi}$, is zero:

$$\det(\mathbf{J}_{\eta\phi}) = l_2 l_3 l_4 l_5 \sin(\phi_2 - \phi_3) \sin(\phi_4 - \phi_5). \quad (19)$$

As the link-lengths are non-zero for the mechanism to exist, Eq. (19) leads to two distinct singularity functions:

$$s_1 \triangleq \sin(\phi_2 - \phi_3), \quad (20)$$

$$s_2 \triangleq \sin(\phi_4 - \phi_5), \quad \text{and} \quad (21)$$

$$s_1 = 0 \Rightarrow \begin{cases} \phi_3 = \phi_2 & \text{or} \\ \phi_3 = \phi_2 \pm k\pi, & k \in \mathbb{Z}^+. \end{cases} \quad (22)$$

$$s_2 = 0 \Rightarrow \begin{cases} \phi_4 = \phi_5 & \text{or} \\ \phi_4 = \phi_5 \pm k\pi, & k \in \mathbb{Z}^+. \end{cases} \quad (23)$$

The signs of the singularity functions identify the kinematic branches of the mechanism uniquely:

- a) Branch UU, if $s_1 < 0$ and $s_2 < 0$.
- b) Branch UD, if $s_1 < 0$ and $s_2 > 0$.
- c) Branch DU, if $s_1 > 0$ and $s_2 < 0$.
- d) Branch DD, if $s_1 > 0$ and $s_2 > 0$.

Here, the first and the second letters in the branch name denote the configuration of abo_2 and cdo_2 chain, respectively: 'U' denotes *elbow up* and 'D' denotes *elbow down* configurations. These have been depicted in Fig. 2.

The singularity function given by s_1 in Eq. (20) represents the singularity in the four-bar loop $o_1abo_2o_1$. Singularity occurs when¹ $\phi_3 = \phi_2 - k\pi$, $k = 0, 1$, geometrically

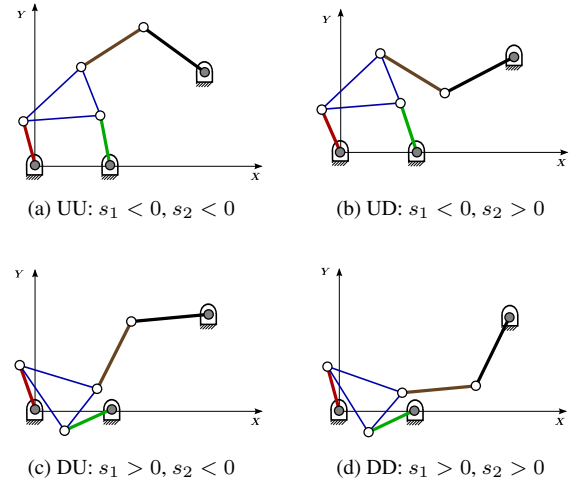


Fig. 2. The four branches of the Stephenson-III mechanism.

equivalent to l_2 and l_3 being collinear. These conditions are depicted in Fig. 3(a) and Fig. 3(b), respectively.

In order to obtain the singularity conditions in terms of architecture parameters, ϕ_3 is eliminated from the Eqs. (7,8) by directly substituting $\phi_3 = \phi_2$ and $\phi_3 = \phi_2 - \pi$. Two different sets of loop-closure equations, namely, $e_1(\theta_1, \phi_2) = (e_{11}, e_{12})^\top = \mathbf{0}$ and $e_2(\theta_1, \phi_2) = (e_{21}, e_{22})^\top = \mathbf{0}$ are obtained, respectively. Solving these specialised loop-closure equations in the same way as described in Section II-A, a non-linear equation only in the input variable θ_1 is derived. The sequential elimination of ϕ_2 and ϕ_3 can be schematically represented as follows:

$$\left. \begin{array}{l} e_{11}(\theta_1, \phi_2) = 0 \\ e_{12}(\theta_1, \phi_2) = 0 \end{array} \right) \xrightarrow{\times \phi_2} h_{1a}(\theta_1) = 0 \xrightarrow{\theta_1 \rightarrow t_1} h_{1b}(t_1) = 0,$$

$$\left. \begin{array}{l} e_{21}(\theta_1, \phi_2) = 0 \\ e_{22}(\theta_1, \phi_2) = 0 \end{array} \right) \xrightarrow{\times \phi_2} h_{2a}(\theta_1) = 0 \xrightarrow{\theta_1 \rightarrow t_1} h_{2b}(t_1) = 0.$$

The equations $h_{1b}(t_1) = 0$ and $h_{2b}(t_1) = 0$ are quadratic in t_1 . For the mechanism to be non-singular, these equations should *not* be satisfied for any $\theta_1 \in [0, 2\pi]$, or equivalently, $t_1 \in \mathbb{R}$. Hence, the discriminants of the two quadratic equations should be negative so that they do not have real roots. The singularity functions, S_1 and S_2 , hence derived, can be written as:

$$S_1 = (l_0 - l_1)^2 - (l_2 - l_3)^2 \text{ from } \phi_3 = \phi_2. \quad (24)$$

$$S_2 = -(l_0 + l_1)^2 + (l_2 + l_3)^2 \text{ from } \phi_3 = \phi_2 - \pi. \quad (25)$$

The singularity functions S_1 and S_2 depend only on architecture parameters, and hence represent characteristics

¹For the singularity condition $s_1 = 0$, $\phi_2 - \phi_3 = \pm k\pi$. Considering $\phi_2 - \phi_3 \in [0, 2\pi]$, $\phi_2 - \phi_3 = 0$ or π .

of the mechanism's architecture—and not of a particular configuration. It is required that the values of these functions are greater than zero for non-singular mechanism. These lead to (an equivalent of) the Grashof's criteria [8], as expected, for the four-bar loop of the mechanism.

The singularity in the loop $o_1acdo_3o_1$ is governed by the function s_2 , and occurs when $\phi_5 = \phi_4 - k\pi$, $k = 0, 1$. This is geometrically equivalent to l_4 and l_5 being collinear, as depicted in Fig. 3(c) and Fig. 3(d), respectively.

Following the same steps used for deriving \mathcal{S}_1 and \mathcal{S}_2 , ϕ_5 is eliminated by substituting $\phi_5 = \phi_4$ and $\phi_5 = \phi_4 - \pi$, respectively, into the constraint equations Eqs. (7–10). Two different sets of loop-closure equations are obtained:

$$\mathbf{k}_1(\theta_1, \phi_2, \phi_3, \phi_4) = (k_{11}, k_{12}, k_{13}, k_{14})^\top = \mathbf{0}, \quad (26)$$

$$\mathbf{k}_2(\theta_1, \phi_2, \phi_3, \phi_4) = (k_{21}, k_{22}, k_{23}, k_{24})^\top = \mathbf{0}. \quad (27)$$

Solving the specialised loop-closure equations $\mathbf{k}_1 = \mathbf{0}$, in the same way as described in Section II-A, a non-linear equation involving only one joint variable, θ_1 is obtained. The sequential elimination of ϕ_2 , ϕ_3 and ϕ_4 can be schematically represented as follows:

$$\left. \begin{array}{l} k_{11}(\theta_1, \phi_{23}) = 0 \\ k_{12}(\theta_1, \phi_{23}) = 0 \\ k_{13}(\theta_1, \phi_{24}) = 0 \\ k_{14}(\theta_1, \phi_{24}) = 0 \end{array} \right\} \begin{array}{l} \xrightarrow{\times \phi_3} q_1(\theta_1, \phi_2) = 0 \\ \xrightarrow{\times \phi_2} q(\theta_1) = 0 \\ \xrightarrow{\times \phi_4} q_2(\theta_1, \phi_2) = 0 \end{array}$$

where, $\phi_{23} = (\phi_2, \phi_3)^\top$ and $\phi_{24} = (\phi_2, \phi_4)^\top$. The function $q(\theta_1)$ is converted into a polynomial using the standard tangent half-angle substitution, $t_1 = \tan \frac{\theta_1}{2}$. This results in a six-degree polynomial in t_1 , whose real solutions give the singular configurations. The six-degree polynomial is of the form $P_{61}(t) = A_1 t^6 + B_1 t^5 + C_1 t^4 + D_1 t^3 + E_1 t^2 + F_1 t + G_1$. Similarly, the condition $\mathbf{k}_2 = \mathbf{0}$ (in Eq. (27)) leads to another six-degree polynomial $P_{62}(t) = A_2 t^6 + B_2 t^5 + C_2 t^4 + D_2 t^3 + E_2 t^2 + F_2 t + G_2$. The coefficients $A_i, \dots, G_i, i = 1, 2$, are independent of the configuration variables and contain only architecture parameters of the mechanism. For the mechanism to be non-singular for all values of $\theta_1 \in [0, 2\pi]$ or equivalently, $t_1 \in \mathbb{R}$, the polynomials P_{61} and P_{62} should not have any real roots. The condition for no real root for any polynomial of even degree can be found as follows. First, it may be observed that:

$$P_n(t) \rightarrow \infty \text{ as } t \rightarrow \pm\infty, \text{ if } A > 0, \quad (28)$$

$$P_n(t) \rightarrow -\infty \text{ as } t \rightarrow \pm\infty, \text{ if } A < 0, \quad (29)$$

where A is the leading coefficient of the polynomial, $P_n(t)$.

Considering the case $A > 0$, for the polynomial $P_n(t)$ to have no real roots, $P_n(t) > 0 \forall t \in \mathbb{R}$. Therefore, the minimum value of the polynomial should be greater than zero. When $A < 0$, for the polynomial $P_n(t)$ not to have any real

root, $P_n(t) < 0 \forall t \in \mathbb{R}$. Therefore, the maximum value of the polynomial $P_n(t)$ should be less than zero. The maximum and the minimum values can be calculated by finding the roots of the derivative of the polynomial and evaluating the polynomials for those values. Thus, the conditions for non-singularity can be written as:

$$\min(P_{61}(t)) > 0, \quad \text{if } A_1 > 0; \quad (30)$$

$$\max(P_{61}(t)) < 0, \quad \text{if } A_1 < 0; \quad (31)$$

$$\min(P_{62}(t)) > 0, \quad \text{if } A_2 > 0; \quad (32)$$

$$\max(P_{62}(t)) < 0, \quad \text{if } A_2 < 0. \quad (33)$$

The singularity functions \mathcal{S}_3 and \mathcal{S}_4 are given by:

$$\mathcal{S}_3 \triangleq \begin{cases} \min(P_{61}(t)), & \text{if } A_1 > 0 \\ -\max(P_{61}(t)), & \text{if } A_1 < 0. \end{cases} \quad (34)$$

$$\mathcal{S}_4 \triangleq \begin{cases} \min(P_{62}(t)), & \text{if } A_2 > 0 \\ -\max(P_{62}(t)), & \text{if } A_2 < 0. \end{cases} \quad (35)$$

The singularity functions $\mathcal{S}_i, i = 1, \dots, 4$ should be greater than zero for the mechanism to be non-singular for full-cycle of the crank. All the four possible singular configurations have been shown in Fig. 3.

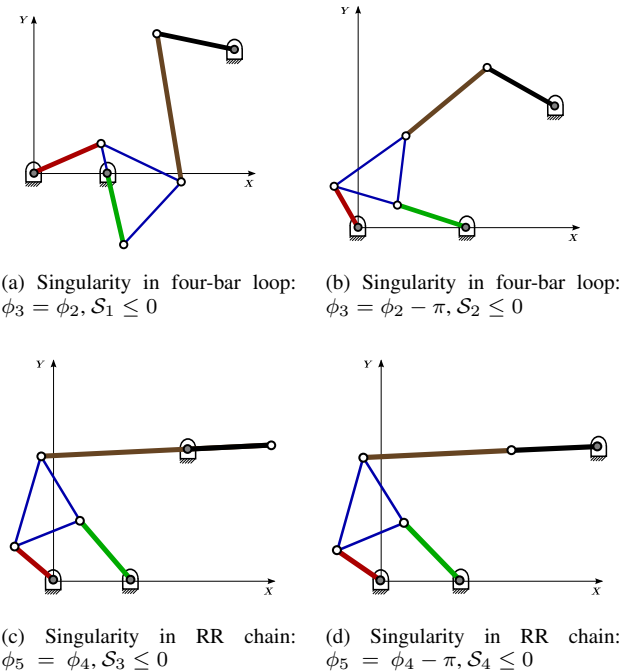


Fig. 3. The geometric representation of the four singularity conditions of the Stephenson-III mechanism. These conditions are mathematically equivalent to singularity conditions $\mathcal{S}_1, \mathcal{S}_2, \mathcal{S}_3$, and \mathcal{S}_4 becoming non-positive, respectively.

C. Assembly criteria

While using a numerical optimisation algorithm, such as *genetic algorithm*, *Cuckoo search*, *differential evolution*, a range for the architecture parameters is specified. Not all combinations in these ranges form a mechanism. Hence, it is important to reject such designs outright without considering them in further computation.

The loop $\mathbf{o}_1\mathbf{acdo}_3\mathbf{o}_1$ can be assembled iff $\forall \theta_1 \in \mathbb{R}$, the distance $\overline{\mathbf{co}_3} \in [|l_4 - l_5|, l_4 + l_5]$:

$$(x - o_{3x})^2 + (y - o_{3y})^2 < (l_4 + l_5)^2, \quad (36)$$

$$(x - o_{3x})^2 + (y - o_{3y})^2 > (l_4 - l_5)^2, \quad (37)$$

where, $x = l_1 \cos \theta_1 + x_c \cos \phi_2 - y_c \sin \phi_2$, and $y = l_1 \sin \theta_1 + x_c \sin \phi_2 + y_c \cos \phi_2$ (see Fig. 1). The two concentric circles, centred at \mathbf{o}_3 and radii of $l_4 + l_5$ and $|l_4 - l_5|$, define the *workspace* of the coupler point \mathbf{c} . On simplification and substitution of the tangent half-angle $t_2 = \tan \frac{\phi_2}{2}$ these inequalities take the form:

$$f_1(\theta_1, t_2) \triangleq A_1 t_2^2 + B_1 t_2 + C_1 < 0, \quad (38)$$

$$f_2(\theta_1, t_2) \triangleq A_2 t_2^2 + B_2 t_2 + C_2 < 0, \quad (39)$$

where the coefficients A_1, B_1, C_1 and A_2, B_2, C_2 are functions of θ_1 , as well as the architecture parameters of the mechanism. Converting the inequalities in Eqs. (38, 39) to equations using the *slack variables* ϵ_1 and ϵ_2 :

$$f_3(\theta_1, t_2) \triangleq A_1 t_2^2 + B_1 t_2 + C_1 + \epsilon_1 = 0, \quad \epsilon_1 > 0, \quad (40)$$

$$f_4(\theta_1, t_2) \triangleq A_2 t_2^2 + B_2 t_2 + C_2 + \epsilon_2 = 0, \quad \epsilon_2 > 0. \quad (41)$$

As the four-bar loop $\mathbf{o}_1\mathbf{abo}_2\mathbf{o}_1$ constrains the angle ϕ_2 in the loop $\mathbf{o}_1\mathbf{acdo}_3\mathbf{o}_1$, the loop-closure equations for four-bar given in Eqs. (7,8) are considered. The angle ϕ_3 is eliminated and using tangent half-angle substitution $t_2 = \tan \frac{\phi_2}{2}$ the constraint equation is derived:

$$f_5(\theta_1, t_2) \triangleq A_3 t_2^2 + B_3 t_2 + C_2 = 0, \quad (42)$$

where the coefficients A_3, B_3, C_3 are functions of θ_1 and architecture parameters of the mechanism. Since Eq. (40) shares common roots with Eq. (42), *resultant* (see, e.g., [15]) of f_3 and f_5 with respect to t_2 is zero:

$$\begin{aligned} & A_3^2 \epsilon_1^2 + (A_1(B_3^2 - 2A_3C_3) + A_3(-B_3B_1 + 2A_3C_1))\epsilon_1 \\ & + A_1^2 C_3^2 + A_1(-B_3B_1C_3 + B_3^2C_1 - 2A_3C_3C_1) \\ & + A_3(B_1^2C_3 - B_3B_1C_1 + A_3C_1^2) = 0. \end{aligned} \quad (43)$$

Similarly, Eq. (41) shares common roots with Eq. (42) and the hence resultant of f_4 and f_5 with respect to t_2 is zero:

$$\begin{aligned} & A_3^2 \epsilon_2^2 + (A_2(B_3^2 - 2A_3C_3) + A_3(-B_3B_2 + 2A_3C_2))\epsilon_2 \\ & + A_2^2 C_3^2 + A_2(-B_3B_2C_3 + B_3^2C_2 - 2A_3C_3C_2) \\ & + A_3(B_2^2C_3 - B_3B_2C_2 + A_3C_2^2) = 0. \end{aligned} \quad (44)$$

The Eqs. (43, 44) are quadratic in ϵ_i : $u_{0i}\epsilon_i^2 + u_{1i}\epsilon_i + u_{2i}$, $i = 1, 2$. As $\epsilon_i > 0$, the roots of the equations should be real and positive. As $u_{0i} = A_3^2 > 0$ for all real A_3 , the condition for the quadratics to have positive real roots can be derived as:

$$\begin{aligned} f_{6i}(\theta_1) = u_{1i} < 0, \quad f_{7i}(\theta_1) = u_{2i} > 0, \\ f_{8i}(\theta_1) = u_{1i}^2 - 4u_{0i}u_{2i} \geq 0, \quad i = 1, 2. \end{aligned} \quad (45)$$

The three constraints, given by Eq. (45), are functions of θ_1 and the architecture parameters. Using tangent half-angle substitution, f_{6i}, f_{7i} , and f_{8i} are converted to polynomials in t_1 . The resulting constraints can be written as:

$$f_{9i}(t_1) < 0, \quad f_{10i}(t_1) > 0, \quad f_{11i}(t_1) \geq 0. \quad (46)$$

The polynomials, f_{9i}, f_{10i} , and f_{11i} , given in Eq. (46), are of degrees 6, 6, and 12 in t_1 , respectively. Following an approach similar to that given in II-B, the conditions obtained on the coefficients of f_{9i} and f_{10i} are:

$$\begin{aligned} A_{f_{9i}} < 0, \quad \max(f_{9i}(t_1)) < 0, \\ A_{f_{10i}} > 0, \quad \min(f_{10i}(t_1)) > 0, \end{aligned}$$

where $A_{f_{9i}}$ and $A_{f_{10i}}$ are the leading coefficients of the polynomials f_{9i} and f_{10i} and $i = 1, 2$. The assembly criteria are now defined as $\mathcal{F}_{ia} > 0$ and $\mathcal{F}_{ib} > 0$, where

$$\mathcal{F}_1 \triangleq \begin{cases} \mathcal{F}_{1a} \triangleq -A_{f_{91}}, \\ \mathcal{F}_{1b} \triangleq -\max(f_{91}(t_1)). \end{cases} \quad (47)$$

$$\mathcal{F}_2 \triangleq \begin{cases} \mathcal{F}_{2a} \triangleq A_{f_{101}}, \\ \mathcal{F}_{2b} \triangleq \min(f_{101}(t_1)). \end{cases} \quad (48)$$

$$\mathcal{F}_3 \triangleq \begin{cases} \mathcal{F}_{3a} \triangleq -A_{f_{92}}, \\ \mathcal{F}_{3b} \triangleq -\max(f_{92}(t_1)). \end{cases} \quad (49)$$

$$\mathcal{F}_4 \triangleq \begin{cases} \mathcal{F}_{4a} \triangleq A_{f_{102}}, \\ \mathcal{F}_{4b} \triangleq \min(f_{102}(t_1)). \end{cases} \quad (50)$$

Each of the polynomials $f_{11i}, i = 1, 2$, factorises into two quadratics and square of a quartic. The square of the quartic is always greater than or equal to 0. The two quadratics correspond to the conditions given by \mathcal{S}_1 and \mathcal{S}_2 , in Eq. (24), and give the following feasibility conditions:

$$\mathcal{F}_5 \triangleq \begin{cases} \mathcal{F}_{5a} \triangleq l_1 + l_2 + l_3 - l_0, \\ \mathcal{F}_{5b} \triangleq l_0 + l_2 + l_3 - l_1. \end{cases} \quad (51)$$

$$\mathcal{F}_6 \triangleq \begin{cases} \mathcal{F}_{6a} \triangleq l_0 + l_1 + l_3 - l_2, \\ \mathcal{F}_{6b} \triangleq l_0 + l_1 + l_2 - l_3. \end{cases} \quad (52)$$

The functions \mathcal{F}_{ia} and $\mathcal{F}_{ib}, i = 1, \dots, 6$ should be greater than 0 so that the mechanism can be assembled $\forall \theta_1 \in [0, 2\pi]$.

Hence, for Stephenson-III mechanism, the conditions for full-cycle mobility are governed by $\mathcal{S}_1, \mathcal{S}_2, \mathcal{S}_3, \mathcal{S}_4, \mathcal{F}_1, \mathcal{F}_2, \mathcal{F}_3, \mathcal{F}_4, \mathcal{F}_5$, and \mathcal{F}_6 . These functions depend only on the architecture parameters.

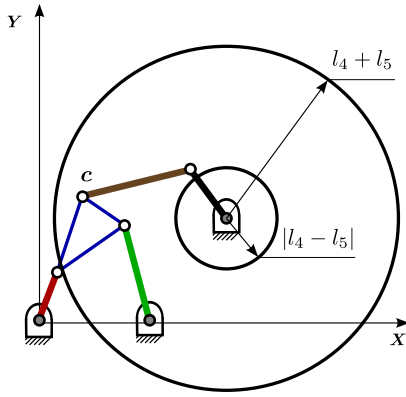


Fig. 4. The two concentric circles, centred at O_3 and radii of $l_4 + l_5$ and $|l_4 - l_5|$, define the workspace of the coupler point c . The assembly criteria are derived from these constraints.

III. Function generation

For the Stephenson-III in Fig. 1, the function generation problem can be stated as:

$$\phi_5(\theta_1) = \phi_{5d}(\theta_1), \quad \theta_1 \in [\theta_{1i}, \theta_{1f}], \quad (53)$$

where $\phi_5(\theta_1)$, and $\phi_{5d}(\theta_1)$ are the *actually generated*, and the *desired* functions, respectively, over $\theta_1 \in [\theta_{1i}, \theta_{1f}]$. This leads to the traditional definition of the (*zeroth order*) *structural error* as:

$$\mathcal{E}_0(\theta_1) = \phi_5(\theta_1) - \phi_{5d}(\theta_1), \quad \theta_1 \in [\theta_{1i}, \theta_{1f}]. \quad (54)$$

In this work, the *first-order structural error* is considered as well. It is defined as the deviation of the derivative of the generated function, from that of the desired one:

$$\begin{aligned} \mathcal{E}_1(\theta_1) &= \frac{d\mathcal{E}_0(\theta_1)}{d\theta_1} = \frac{d\phi_5(\theta_1)}{d\theta_1} - \frac{d\phi_{5d}(\theta_1)}{d\theta_1} \\ &= K_{\phi_5\theta_1}(\theta_1) - \frac{d\phi_{5d}(\theta_1)}{d\theta_1}, \quad \theta_1 \in [\theta_{1i}, \theta_{1f}], \end{aligned} \quad (55)$$

where $K_{\phi_5\theta_1}(\theta_1)$ is the velocity coefficient as in Eq. (16).

Minimisation of the maximum zeroth-order structural error (over the specified range of motion) leads to a mechanism in which the absolute value of the structural error is *bounded* by some upper limit. However, an objective considering only this aspect is *insensitive* to the variation of the error function within this bound. For instance, as shown in Fig. 5, both the cases (a) and (b) would lead to the same objective value, whereas case (b) is clearly more desirable, since it would lead to lesser unwanted oscillations in the resulting mechanism. It is easy to see that the first-order error measure would be able to mitigate these oscillations, by reducing the variation in the error function. However, this measure, by itself, is insensitive to a “DC-shift”, i.e., a constant error, however large. Therefore, it is appealing to use both these measures together, in what may be termed as a *dual-order* formulation of the structural error. This has

been done in the present work by means of a multi-objective formulation of the synthesis problem, in which each objective relates to the error in a different order. To the best of the knowledge of the authors, such a formulation is entirely novel.

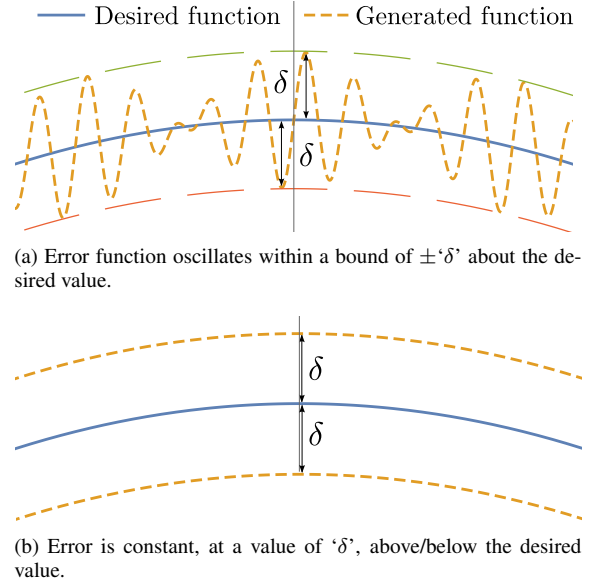


Fig. 5. Types of errors in function generation and their implications.

A. Synthesis of function generator as an optimisation problem

An optimisation problem with constraints can be mathematically expressed as:

$$\begin{aligned} &\text{Minimise} && F_i(\mathbf{x}), \quad i = 1, 2, \dots, p \\ &\text{subject to} && G_j(\mathbf{x}) \geq 0, \quad j = 1, 2, \dots, q; \\ &&& H_k(\mathbf{x}) = 0, \quad k = 1, 2, \dots, r; \\ &&& x_l \in [a_l, b_l], \quad l = 1, 2, \dots, w, \end{aligned} \quad (56)$$

where $F_i(\mathbf{x})$ are the objective functions, $\mathbf{x} = (x_1, \dots, x_l)^\top$ is the vector of design variables, with x_l bounded between a_l and b_l . The inequality and equality constraint functions are represented by $G_j(\mathbf{x})$ and $H_k(\mathbf{x})$, respectively. A maximisation objective can be converted to a minimisation objective by negating it. For the function generation problem of Stephenson-III mechanism, given by Eq. (53), the error in the zeroth and first order functions are given by Eq. (54) and Eq. (55).

The design variables are the architecture parameters: $\mathbf{x} = (l_0, l_2, l_3, l_4, l_5, x_c, y_c, b_{3x}, b_{3y})^\top$. Without any loss of generality, the link lengths are normalised with respect to l_1 . The mobility criteria, governed by the functions $\mathcal{S}_i, i = 1, \dots, 4$ and $\mathcal{F}_i, i = 1, \dots, 6$, described in Section II, form the constraints. The span of the input joint variable θ_1 was divided into N sample points. Roots of the

FKU equation represent the branches of the position kinematics for a given value of θ_1 . The branches are distinguished on the basis of the sign of singularity functions, as discussed in Section II-B. The mobility criteria ensure that all the four branches can be assembled, and are free from singularities. The numerical optimisation, as described below, is performed on each branch independently, thereby eliminating the possibility of the existence of branch-errors in the solutions obtained. This also ensures exhaustive coverage of *all* the potential solutions across all the branches.

The dual order function generation problem can be mathematically expressed as:

$$\begin{aligned} \text{Minimise } F_1 &\triangleq \frac{1}{N} \sum_{j=1}^N \mathcal{E}_0^2(\theta_{1j}), \\ F_2 &\triangleq \frac{1}{N} \sum_{j=1}^N \mathcal{E}_1^2(\theta_{1j}), \\ \text{where, } \theta_{1j} &\in [\theta_{1i}, \theta_{1f}]; \\ \text{subject to } G_{S_p}(\mathbf{x}) &\triangleq S_p > 0, \\ G_{\mathcal{F}_q}(\mathbf{x}) &\triangleq \begin{cases} \mathcal{F}_{qa} > 0, \\ \mathcal{F}_{qb} > 0, \end{cases} \\ \text{where, } p &= 1, \dots, 4, \quad q = 1, \dots, 6, \\ x_l \in [a_l, b_l], \quad l &= 1, \dots, 9. \end{aligned} \quad (57)$$

IV. Numerical studies

The above formulation of optimal design of Stephenson-III for function generation is applied to two functions previously studied in literature:

1. A parabolic function, originally used by McLarnan in [12], and revisited in [3].
2. Double dwell function given in [13], and used as a benchmark in [14].

The function generation problem is posed as an optimisation problem, and is implemented using NSGA-II² [11]. In the sections below, the various desired functions are described and the results are given.

A. Parabolic function

The function generation problem is defined by the parabolic function given as:

$$\phi_{5d}(\theta_1) = \frac{\theta_1^2}{90}, \quad \text{where all angles are in degrees.} \quad (58)$$

The RMS value of the error functions, described in Eqs. (54, 55), form the objective functions in the optimisation problem and the mobility criteria form the constraints. The bounds of the design variables, \mathbf{x} , are given in Table I.

TABLE I. Variable bounds for design variables in parabola function generation ($x_l \in [a_l, b_l]$)

x_l	l_0	l_2	l_3	l_4	l_5	x_c	y_c	o_{3x}	o_{3y}
a_l	1	1	1	1	1	0	0	1	0
b_l	6	6	6	6	6	3.5	5	8	3.5

In order to facilitate compactness and easy manufacturing of the mechanism, ratio of the link lengths were taken to satisfy $(\max k_j / \min k_j) \leq 6, j = 1, \dots, 8$ where k_j comprise the parameters $l_i, i = 0, \dots, 5$ and also the lengths of the three sides of the coupler link. The maximum ratio of the link lengths is considered to be 6, following [16]. The number of sample points, N , is taken to be 400, resulting in a resolution of 0.225° for the input angle, θ_1 . The NSGA-II optimisation was carried out for a *population* size of 2000 over 1000 *generations*, which took 12 min to cover all the branches³. Seven design solutions were obtained. From the *Pareto plot* (see, e.g., [17]), the designer is free to choose the preferred solution based on the application and tolerance limits. The solution with the minimum zeroth order error appeared in the branch DU. This particular solution has been used in the numerical results tabulated below. The architecture parameters obtained have been reported in Table II. The errors are reported and compared with [3] in Table III. It is observed that, while the structural error in [3] is lower than the results obtained, they are of the same order of magnitude. Figure 6 shows the mechanism for parabola function generation. The desired function, generated function, and dual-order errors are shown in Fig. 7.

TABLE II. Results: architecture parameters for parabolic function

l_0	5.78446	l_5	3.51675
l_1	1	x_c	3.12342
l_2	1.33374	y_c	1.37407
l_3	5.61890	o_{3x}	0.98506
l_4	4.88862	o_{3y}	-0.60812

TABLE III. Results and comparison with [3] for parabolic function

Present work		From [3]	
$\max \mathcal{E}_0(\theta_1) $	0.04208°	$\max \mathcal{E}_0(\theta_1) $	0.0245°
RMS ($\mathcal{E}_0(\theta_1)$)	0.02598°		
$\max \mathcal{E}_1(\theta_1) $	0.02313		
RMS ($\mathcal{E}_1(\theta_1)$)	0.00507		

B. Double dwell as a function generation problem

The design of a six-bar mechanism having double dwell at specified locations of the output link is a standard prob-

²NSGA-II is available for free from the Kanpur Genetic Algorithms Laboratory at <http://www.iitk.ac.in/kangal/codes.shtml>.

³PC configuration: Intel core i7-4770 CPU running at 3.40 GHz with 8 GB RAM.

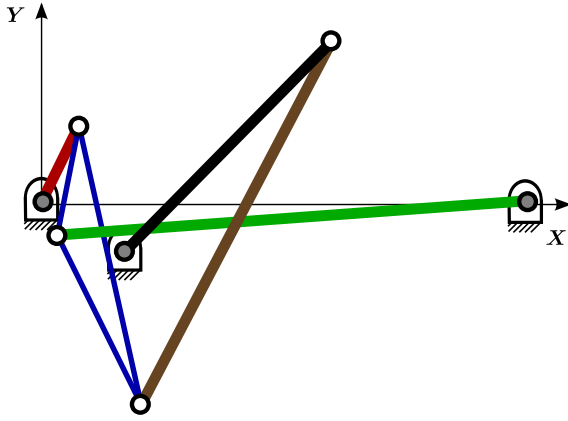


Fig. 6. The mechanism for parabola function generation.

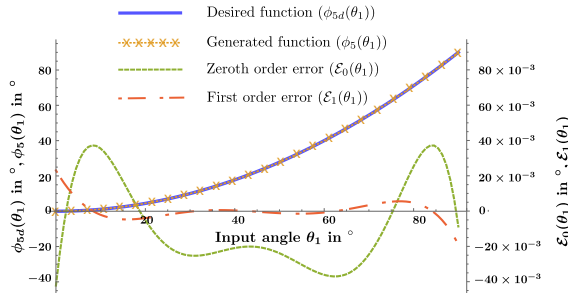


Fig. 7. The desired function, generated function, and errors in zeroth and first order.

lem and has been studied in [13], [14], [16] recently via optimisation. The above formulation is applied to revisit the problem. The double dwell problem is described as follows:

$$\phi_5(\theta_1) = \begin{cases} \phi_5 = \phi_{51} & \forall \theta_1 \in [-15^\circ, 15^\circ], \\ \phi_5 = \phi_{52} & \forall \theta_1 \in [160^\circ, 220^\circ], \end{cases} \quad (59)$$

where ϕ_{51} and ϕ_{52} are the desired dwell output angles. The span of θ_1 is divided into $N_1 = 100$ and $N_2 = 400$ sample points for first and second dwell respectively. The desired values of ϕ_5 at the first and second dwell are $\phi_{51} = 225^\circ$ and $\phi_{52} = 210^\circ$, respectively. The full cycle mobility conditions are used as constraints. The design problem is to find the set of architecture parameters such that the double dwell is achieved optimising dual order objective functions and satisfying mobility criteria. The variable bounds of the design variables are given in Table IV (adopted from [14]).

TABLE IV. Variable bounds for design variables in double dwell problem ($x_l \in [a_l, b_l]$)

x_l	l_0	l_2	l_3	l_4	l_5	x_c	y_c	o_{3x}	o_{3y}
a_l	1	1	1	1	1	0	-3.5	1	-3
b_l	5	5	5	5	5	3.5	0	8	-1

A total of 34 solutions were obtained. Architecture parameters of the design corresponding to the *utopia* point (see, e.g., [17]) is given in Table V. The errors in the zeroth and first order, and a comparison with [13] and [14] are given in Table VI. It is observed that the results are of *one* order of magnitude better than [13] and comparable to [14]. However, in [14] the first and the second dwell occur at $\phi_5 = 114.63^\circ$ and $\phi_5 = 125.28^\circ$, respectively, as opposed to the two specific locations, $\phi_5 = 225^\circ$ and $\phi_5 = 210^\circ$, as in this case. The schematic of the mechanism is shown in Fig. 10.

TABLE V. Results: architecture parameters for double dwell function generation

l_0	2.18080	l_5	2.00476
l_1	1	x_c	1.27544
l_2	1.62927	y_c	0.94626
l_3	1.93324	o_{3x}	5.70579
l_4	4.97792	o_{3y}	-0.01524

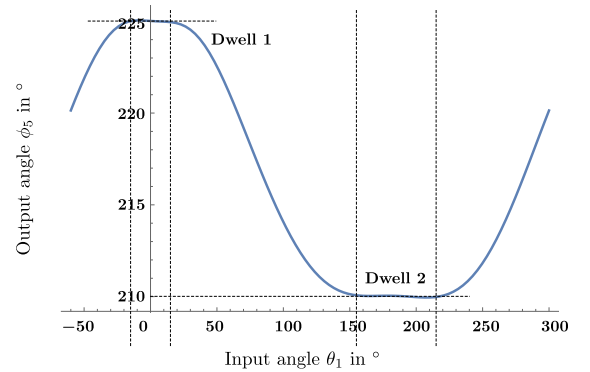
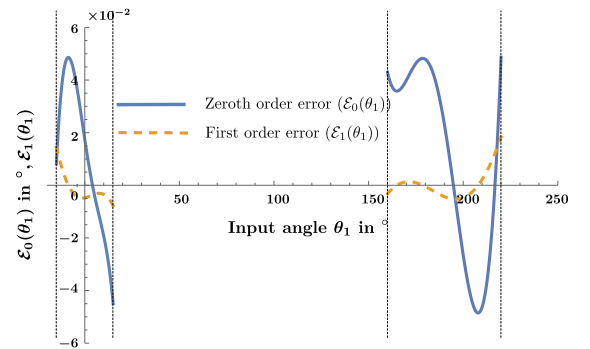
Fig. 8. Plot of the output angle ϕ_5 for the full cycle of input angle, θ_1 for double dwell function generation.

Fig. 9. Zeroth order and first order errors for double dwell function generation.

TABLE VI. Results and comparison with [13] and [14] for double dwell function generation

Dwell Period	Error	Present work	Calculated from [13]	^a Calculated from [14]
$\theta_1 \in [-15^\circ, 15^\circ]$ $\phi_{51} = 225^\circ$	$\max \mathcal{E}_0(\theta_1) $ (in $^\circ$)	0.04860	0.55610	0.04412
	RMS ($\mathcal{E}_0(\theta_1)$) (in $^\circ$)	0.03023	0.27447	-
	$\max (\mathcal{E}_1(\theta_1))$	0.01445	0.05326	0.01419
	RMS ($\mathcal{E}_1(\theta_1)$)	0.00519	0.04031	0.00518
$\theta_1 \in [160^\circ, 220^\circ]$ $\phi_{52} = 210^\circ$	$\max \mathcal{E}_0(\theta_1) $ (in $^\circ$)	0.04863	0.25444	0.08468
	RMS ($\mathcal{E}_0(\theta_1)$) (in $^\circ$)	0.03974	0.10163	-
	$\max (\mathcal{E}_1(\theta_1))$	0.01828	0.03137	0.00612
	RMS ($\mathcal{E}_1(\theta_1)$)	0.00511	0.01199	0.00235

^a In [14] the first and the second dwell occur at $\phi_5 = 114.63^\circ$ and $\phi_5 = 125.28^\circ$, respectively. The zeroth order error is calculated as the difference between maximum and minimum value of the generated output in the respective ranges of the dwell motions in this case.

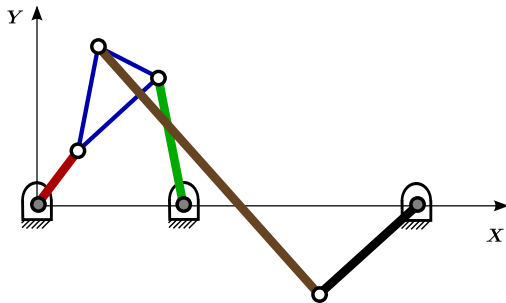


Fig. 10. The mechanism for double dwell function generation.

V. Conclusions

A new formulation for the optimal design of a six-bar function generator has been presented in this paper. Several new concepts related to the mobility analysis, as well as the formulation of a multi-objective optimisation problem using the dual-order structural error have been introduced. The derivations and the corresponding results have been demonstrated via application to a Stephenson-III mechanism. Numerical studies were carried out for two function generation problems—(a) parabolic function and, (b) double-dwell function. The results obtained were comparable to that of the exact 8 precision-point synthesis in the case of the parabolic function. In the case of the double-dwell problem, the obtained results represent an improvement over those reported in existing literature. The proposed formulation is applicable to other single-degree-of-freedom mechanisms, including six-bar mechanisms of the other topologies. Analysis of these would be one of the future extensions of the present work.

References

- [1] F. Freudenstein, "An analytical approach to the design of four-link mechanisms," *Transactions of the ASME*, vol. 76, pp. 483–492, 1954.
- [2] S. Antonin, "Mechanism for use in computing apparatus," Aug. 31 1943, US Patent 2,328,306.
- [3] M. M. Plecnik and J. M. McCarthy, "Numerical synthesis of six-bar linkages for mechanical computation," *Journal of Mechanisms and Robotics*, vol. 6, no. 3, p. 031012, 2014.
- [4] D. J. Bates, J. D. Hauenstein, A. J. Sommese, and C. W. Wampler, "Bertini: Software for numerical algebraic geometry," Available at bertini.nd.edu.
- [5] S. Acharyya and M. Mandal, "Performance of EAs for four-bar linkage synthesis," *Mechanism and Machine Theory*, vol. 44, no. 9, pp. 1784–1794, 2009.
- [6] W.-Y. Lin, "A GA-DE hybrid evolutionary algorithm for path synthesis of four-bar linkage," *Mechanism and Machine Theory*, vol. 45, no. 8, pp. 1096–1107, 2010.
- [7] C. W. Wampler, A. P. Morgan, and A. J. Sommese, "Complete solution of the nine-point path synthesis problem for four-bar linkages," *Journal of Mechanical Design*, vol. 114, pp. 153–159, 1992.
- [8] F. Grashof, *Theoretische maschinenlehre*. L. Voss, 1890, no. v. 3.
- [9] R. Srivatsan and S. Bandyopadhyay, "Analysis of constraint equations and their singularities," in *Advances in Robot Kinematics*, J. Lenarčič and O. Khatib, Eds. Springer International Publishing, 2014, pp. 429–436.
- [10] S. Bandyopadhyay and A. Ghosal, "Analysis of configuration space singularities of closed-loop mechanisms and parallel manipulators," *Mechanism and Machine Theory*, vol. 39, no. 5, pp. 519–544, 2004.
- [11] K. Deb, S. Agrawal, A. Pratap, and T. Meyarivan, "A fast and elitist multi-objective genetic algorithm: NSGA-II," *IEEE Transactions on Evolutionary Computation*, vol. 6, no. 2, pp. 182–197, 2002.
- [12] C. W. McLarnan, "Synthesis of six-link plane mechanisms by numerical analysis," *Journal of Manufacturing Science and Engineering*, vol. 85, 1963.
- [13] P. Shiakolas, D. Koladiya, and J. Kiebler, "On the optimum synthesis of six-bar linkages using differential evolution and the geometric centroid of precision positions technique," *Mechanism and Machine Theory*, vol. 40, no. 3, pp. 319–335, 2005.
- [14] M. Jagannath and S. Bandyopadhyay, "A new approach towards the synthesis of six-bar double dwell mechanisms," in *Computational Kinematics*, A. Kecskeméthy and A. Müller, Eds. Springer Berlin Heidelberg, 2009, pp. 209–216.
- [15] D. Cox, J. Little, and D. O'Shea, *Ideals, Varieties, and Algorithms: An Introduction to Computational Algebraic Geometry and Commutative Algebra*. New York: Springer-Verlag, 1991.
- [16] R. R. Bulatović, S. R. Dordević, and V. S. Dordević, "Cuckoo search algorithm: a metaheuristic approach to solving the problem of optimum synthesis of a six-bar double dwell linkage," *Mechanism and Machine Theory*, vol. 61, pp. 1–13, 2013.
- [17] K. Deb, *Multi-Objective Optimization Using Evolutionary Algorithms*, ser. Wiley Interscience Series in Systems and Optimization. Wiley, 2001.